A density-functional theory investigation of the electronic structure of the active carbon graphite-like and amorphous domains

ARTICLE *in* CHEMICAL PHYSICS LETTERS · SEPTEMBER 2011

Impact Factor: 1.9 · DOI: 10.1016/j.cplett.2011.08.009

4 AUTHORS, INCLUDING:

Oleksiy V. Khavryuchenko

40 PUBLICATIONS **184** CITATIONS

SEE PROFILE

Volodymyr Khavryuchenko

18 PUBLICATIONS **98** CITATIONS

SEE PROFILE

Vladyslav V Lisnyak

National Taras Shevchenko University of Kyiv

124 PUBLICATIONS **354** CITATIONS

SEE PROFILE

Chemical Physics Letters 513 (2011) 261–266

Contents lists available at SciVerse ScienceDirect

Chemical Physics Letters

journal homepage: www.elsevier.com/locate/cplett

A density-functional theory investigation of the electronic structure of the active carbon graphite-like and amorphous domains

Oleksiy V. Khavryuchenko [a,c,*], Volodymyr D. Khavryuchenko [b], Vladyslav V. Lisnyak [a], Gilles H. Peslherbe [c]

[a] Chemical Department, Kyiv National Taras Shevchenko University, 64 Volodymyrska Str., UA-01601 Kyiv, Ukraine
[b] Institute for Sorption and Problems of Endoecology, National Academy of Sciences of Ukraine, 13 General Naumov Str., UA-03167 Kyiv, Ukraine
[c] Centre for Research in Molecular Modeling and Department of Chemistry and Biochemistry, Concordia University, Montréal, QC, Canada H4B1R6

ARTICLE INFO

Article history:
Received 3 May 2011
In final form 7 August 2011
Available online 10 August 2011

ABSTRACT

The electronic structure of model clusters of the graphite-like and disordered amorphous domains of active carbon has been calculated with density-functional theory (B3LYP/SVP). Structural transformations of amorphous clusters are observed upon change of multiplicity, and high-multiplicity states are found to be the most stable. Spin-active centers tend to form conjugated chains with an electronic structure made up of non-interacting singly-occupied orbitals.

1. Introduction

The traditional picture of the active carbon (AC) structure is based on the concepts of non-graphitizable carbon [1,2] and turbostratic graphite [3,4], and it was recently modified in light of the discovery of curved graphene planes [5,6]. In this paradigm, the surface chemical properties of the AC reduce to the properties of the unsaturated edge carbon atoms and of the organic functional groups (−COOH, −OH, −CHO, etc.) grafted on the edges [7]. However, the smooth character of the acid/base properties [7] is not consistent with the ordinary pK_a values of the organic functional groups. Furthermore, the mechanical hardness of the AC cannot be explained simply by van der Waals interactions between graphene sheets. Finally, there is spectroscopic evidence that the AC contains a large amount of sp^3-hybridized carbon [8,9]. All these findings lead to an updated picture of the AC structure, which would contain two major domains, a graphite-like domain and a disordered amorphous one [10,11].

Establishing a comprehensive model of AC and computing its properties is an intense area of research, due to the wide application of carbon materials and their practical importance. However, the majority of such models are still based solely on ordered graphite-like clusters [2,12,13] or non-bonded curved carbon sheets [14,15]. Moreover, structural investigations of AC have been limited to the mesoscopic scale, and have focused, for instance, on the mutual orientation of micro- and submicro-sized particles inside the bulk [2,12,15]; a full atomistic picture has yet to be provided. The main obstacle in the description of the AC structure lies in its amorphous character. The traditional approach to investigate periodic solids can hardly be used for completely amorphous solids such as glasses or non-graphitizable carbon, and a single structural model of AC would not be representative of the distribution of atomic configurations in the amorphous material [16].

Another aspect of the AC chemistry, which is often overlooked, is the dependence of the chemical and physical properties of the material under consideration on its spin state (i.e. multiplicity). Recent semiempirical PM3 and *ab initio* Hartree–Fock quantum–chemical calculations of the carbonization of the polystyrene–divinylbenzene (PSDVB) copolymer [17–19] exhibits that the amorphous domain of AC possesses stable states with non-zero spin magnetic moment M_S [20][1], as was also found for large polyaromatic hydrocarbon (PAH) clusters [22–25]. This greatly affects the electronic and, thus, chemical properties of AC and might be considered a unique feature of pure-carbon chemistry, distinguishing it from ordinary organic chemistry. In this Letter, we report and discuss the results of density-functional theory calculations of the electronic structure and spin properties of both graphite-like and disordered carbon clusters, as models of the postulated two major domains of AC.

2. Methodology

Quantum–chemical calculations were performed with the cluster (supermolecular) approach in the framework of density-functional theory (DFT) with the hybrid three-parameter Becke Lee–Yang–Parr functional (B3LYP) [26] as implemented in the ORCA program [27], together with Ahlrichs' double-zeta split-valence basis set augmented by polarization functions (SVP) [28]. A few calculations were also performed with the Becke–Perdew 86

* Corresponding author at: Chemical Department, Kyiv National Taras Shevchenko University, 64 Volodymyrska Str., UA-01601 Kyiv, Ukraine. Fax: +38 044 25 81 241.
E-mail addresses: oleksiy@cermm.concordia.ca, alexk@univ.kiev.ua (Oleksiy V. Khavryuchenko).

[1] We note that the spin magnetic moment M_s is also sometimes denoted as S_z [21].

0009-2614/$ - see front matter © 2011 Elsevier B.V. All rights reserved.
doi:10.1016/j.cplett.2011.08.009

(BP86) functional [29,30] and the def2-SVP basis set [31] to assess the robustness of the computed results with respect to the choice of functional and basis set. The restricted Kohn–Sham (RKS) method was employed for closed-shell singlet states, while the unrestricted Kohn–Sham (UKS) method was employed for higher-multiplicity (M_s = 1–6) open-shell states. The broken-symmetry (BS) singlet state was calculated with the UKS method for all clusters by using the electron density matrix of the most stable high-multiplicity state as the initial density matrix in the calculations (although some other non-diagonal initial electron density matrices sometimes led to the same solution).

Since some amorphous clusters appeared to undergo spontaneous, irreversible, intramolecular structural transformations in certain multiplicity states (as will be discussed in Section 4), the energy of such states was evaluated for the geometry of the most stable spin state (i.e. without geometry optimization), and these results should be treated with care. For the remainder of the clusters, the geometries were fully optimized and the energies, extent of spin contamination and spin density distributions were evaluated for the optimized geometries (*cf.* Supplemental Information A for computational protocols and Cartesian coordinates of all cluster structures). The extent of spin contamination was evaluated as the difference between the calculated expectation value $< S^2 >$ and the theoretical $S\cdot(S+1)$ value for each state. Spin density distributions were visualized with the UCSF Chimera package [32] (*cf.* Supplemental Information B for additional illustrations).

3. Results

Figure 1 displays the carbon structures considered in this Letter. The $C_{96}H_{18}$ PAH, shown in Figure 1A and derived from the hexagulene $C_{96}H_{24}$ [22] by eliminating the hydrogen atoms from one edge of the cluster, is considered as a model of the graphite-like domain of AC, while the $C_{92}H_{24}$ structures **1** to **4**, shown in Figure 1B, are considered as models of the amorphous domain. It should be emphasized that the amorphous cluster structures are not unique and should only be considered as representative of a distribution of possible atomic configurations. Structure **1** was taken from previously reported PM3 calculations [20,33]; it undergoes spontaneous, irreversible, intramolecular structural transformation into **2** by reaction of two neighboring unsaturated carbon atoms in states of multiplicity 7, 9, 11, and 13, while it converts into **3** in the RKS singlet state or into **4** in the triplet state (*cf.* Figure 1B). Moreover, **2** also converts into **3** in the BS singlet state.

The triplet state (M_s = 1) is the most stable state for the $C_{96}H_{18}$ cluster (*cf.* Table 1). However, the energy difference between the triplet state and the BS singlet state is negligible (0.4 kcal/mol), and these two states will be analyzed together. As for the four structural isomers of the amorphous cluster, the data collected in Table 1 and plotted in Figure 2 show that they all behave analogously with respect to stability *vs.* multiplicity: the B3LYP/SVP energies of the high-multiplicity states are close and much lower than that of the singlet state by *ca.* 90–100 kcal/mol. We note that the latter is much less than the stabilization energy predicted by PM3 [34,35] and HF/6-31G [36,37] (~310 and 575 kcal/mol, respectively) [20], but it is still quite substantial. For instance, the energies of **2** with M_s = 1, 3, 4, and 5, as well as that of the BS singlet state, differ by no more than 7 kcal/mol and are lower than that of the singlet state by *ca.* 90 kcal/mol. Thus, the high-multiplicity spin-polarized states are quasi-degenerate and they constitute the most stable electronic states of the amorphous clusters. Additional BP86/SVP and B3LYP/def2-SVP calculations for **3** lead

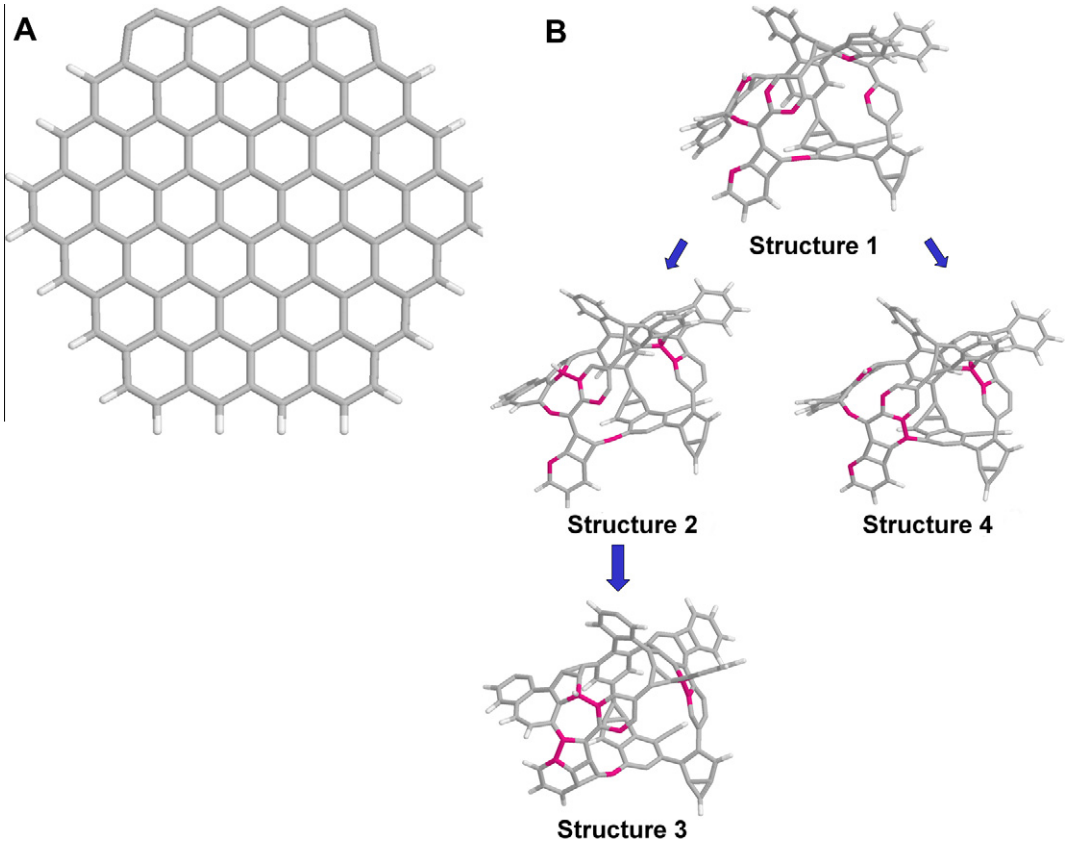

Figure 1. B3LYP/SVP optimized geometries of (A) $C_{96}H_{18}$ and (B) the $C_{92}H_{24}$ amorphous carbon models **1** to **4**. Structural transformations upon change of multiplicity are illustrated with the carbon atoms forming new bonds shown in pink for clarity. (For interpretation of the references in colour in this figure legend, the reader is referred to the web version of this article.)

Table 1
B3LYP/SVP results for all carbon structures.

	Multiplicity	Relative energy[a]
$C_{96}H_{18}$	1 (RKS)	0
	3	−27.4
	5	3.0
	7	34.6
	1 (UKS)[b]	−0.02
	1 (UKS)[c]	−27.0
Structure **1**	1 (RKS)[d]	0.000
	3[d]	−91.6
	5	−91.8
	7[d]	−96.2
	9[d]	−80.4
	11[d]	−63.6
	13[d]	−24.9
	1 (UKS)[d,e]	−91.7
Structure **2**	1 (RKS)	−62.5
	3	−157.6
	5	−156.7
	7	−156.0
	9	−159.6
	11	−159.7
	13	−130.1
	1 (UKS)[d,f]	−157.6
Structure **3**	1 (RKS)	−111.0
	3	−204.5
	5	−211.4
	7	−211.6
	9	−181.8
	11	−184.7
	13	−143.4
	1 (UKS)[g]	−205.3
Structure **4**	1 (RKS)[d]	−109.6
	3	−220.3
	5	−218.7
	7	−219.9
	9	−219.4
	11	−188.1
	13	−143.4
	1 (UKS)[h]	−220.3
Structure **2H**[j]	1 (RKS)	0
	3	0.6
	5	0.8
	7	1.0
	9	1.6
	11	12.1
	13	73.3
	1 (UKS)[i]	1.6

[a] Relative energy (in kcal/mol) with respect to the RKS singlet state (the RKS singlet state of **1** serves as a reference for all amorphous cluster isomers **1**–**4**).
[b] Calculated with an initial diagonal electron density matrix.
[c] Calculated with an initial electron density matrix from the solution for the $M_s = 1$ state.
[d] Without geometry relaxation (see text for details).
[e] Calculated with an initial electron density matrix from the solution for the $M_s = 2$ state.
[f] Calculated with an initial electron density matrix from the solution for the $M_s = 4$ state.
[g] Calculated with an initial electron density matrix from the solution for the $M_s = 3$ state.
[h] Calculated with an initial electron density matrix from the solution for the $M_s = 1$ state.
[i] Calculated with an initial electron density matrix from the solution for the $M_s = 4$ state.
[j] Structure **2** with one sp^2-hybridized, twofold coordinated carbon atom in the middle of the spin chain saturated with two H atoms (refer to Figure 4).

to analogous results (*cf.* Supplemental Information D). In the remainder of the Letter, unless otherwise specified, **2** will be discussed as a paradigm for the amorphous clusters, but similar conclusions apply to the other structures.

The extent of spin contamination in the present calculations is relatively high (*cf.* Supplemental Information C). The concept of spin contamination is not well defined in DFT [38] and it is still a point of debate [21,39,40]; nevertheless, its extent has been used in some cases as a source of information about the electronic structure of the system, a classical example being H_2 dissociation [21]. The extent of spin contamination has also been shown to reflect the antiferromagnetic nature of systems such as di–iron–oxo proteins; in their BS singlet state [21,39], with two iron(III) nuclei coupled through non-magnetic O^{2-} or OH^- bridges, this system possesses five α-spin electrons and five β-spin electrons occupying non-overlapping orbitals, thus forming an antiferromagnetic system, with an extent of spin contamination of *ca.* 5. Single-determinant DFT results should obviously be treated with caution for systems with electronic multi-configuration character such as polyradicals, but no matter how imperfect, the approach has been shown to be valid if the energies of the different electronic configurations are close and within the error of the method itself [41]. In the present calculations, the estimated corrections [42–44] to the pure singlet state energies are small (*e.g.* 1.5 kcal/mol for **1**, 0.4 kcal/mol for $C_{96}H_{18}$, and −0.255 kcal/mol for **4**) and certainly within the error of the computations. Therefore, spin contamination has a negligible effect on the energy of the systems considered here and it does not affect the validity of the present results.

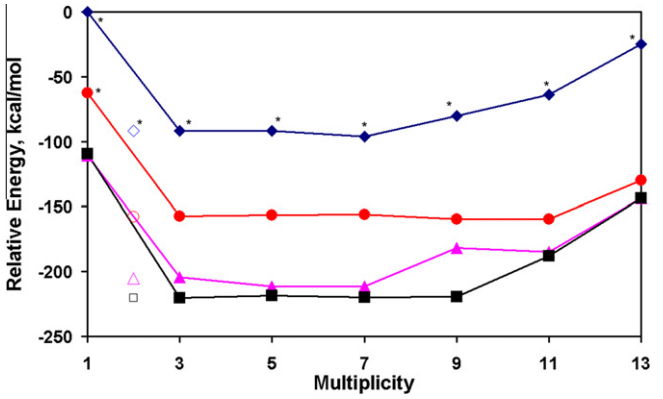

Figure 2. B3LYP/SVP relative energy of the amorphous carbon models *vs.* multiplicity. The dots denote BS open-shell singlet-state energies. Energies calculated for structures without geometry relaxation are marked with an asterisk. (diamonds: **1**, circles: **2**, triangles: **3**, squares: **4**).

The B3LYP/SVP energy gaps between the highest occupied molecular orbital (HOMO) and the lowest unoccupied molecular orbital (LUMO) are much lower than those previously predicted by the Hartree–Fock method [20] (*cf.* Supplemental Information C) for all structures. This is not a surprising result, since DFT has been reported to often narrow the HOMO/LUMO gaps [45]). For $C_{96}H_{18}$ and the **1** to **4** clusters in their most stable multiplicity states, the values of the HOMO/LUMO gaps vary over a rather narrow range of *ca.* 0.9–2.5 eV, with the majority in the range 1.3–2.0 eV. On the other hand, the HOMO/LUMO gap decreases drastically to 0.35–0.45 eV in the RKS singlet state, as observed previously [20]. This could suggest serious deviations from linear response in the electric and magnetic properties of AC.

4. Discussion

The discussion of the results will focus on (1) the origin and the consequences of the structural transformations in the amorphous domain, (2) the structural motifs, related to the stability of high-multiplicity states in all models, (3) the nature of the BS open-shell singlet state, and (4) the impact of the stability of high-multiplicity states on the chemical properties of AC.

Being post-polymeric constructs [20,33], the amorphous clusters partially retain the flexibility of the polymer chains, although they

are more tightly interconnected due to deep carbonization. As a consequence, the geometry of the amorphous domain is more sensitive to electron-density relocalization, caused by changes in spin state, and the clusters can easily relax to more energetically favorable conformations. Structure **3**, which results from interconversion of **1** and/or **2**, includes a fragment of 9 condensed (three- to seven-membered) carbon rings, which might be considered a precursor of a curved graphene-like surface. Hence, transformation of a polymer to a pre-graphitic structure occurs spontaneously upon spin-state change and geometry relaxation. Since reactions between unsaturated carbon atoms in amorphous clusters are energetically favorable, thermal fluctuations could lead to less defective structures such as graphene-like sheets. However, it is important to note that the spin state is an essential factor for such conjugated disordered systems, as spin-state changes can spontaneously drive crucial structural transformations, even at very low temperature.

The spin density of the most stable triplet and BS singlet states of $C_{96}H_{18}$ is, not surprisingly, localized on the unsaturated edge, i.e. on the sp^2-hybridized, twofold coordinated, carbon atoms (*cf.* Figure 3). The spin density distribution for the amorphous clusters (*cf.* Figure 4 for the paradigm structure **2** and Supplemental Information B for other structures) is much more convoluted. One may distinguish six types of functional elements in the structure of the clusters with respect to spin properties: (1) sp^2-hybridized, twofold coordinated, carbon atoms (both endocyclic and exocyclic), (2) slightly pyramidalized threefold coordinated carbon atoms, (3) polyyne chains,

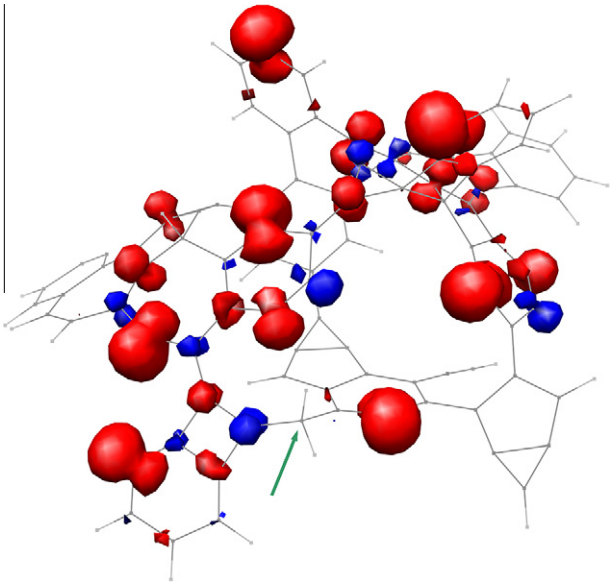

Figure 4. Spin density distribution of the multiplicity 9 structure **2H**. The spin chain cleavage site is indicated by an arrow for clarity. The α-spin density is shown in red and the β-spin density in blue. Isosurface level – 0.01. (For interpretation of the references in colour in this figure legend, the reader is referred to the web version of this article.)

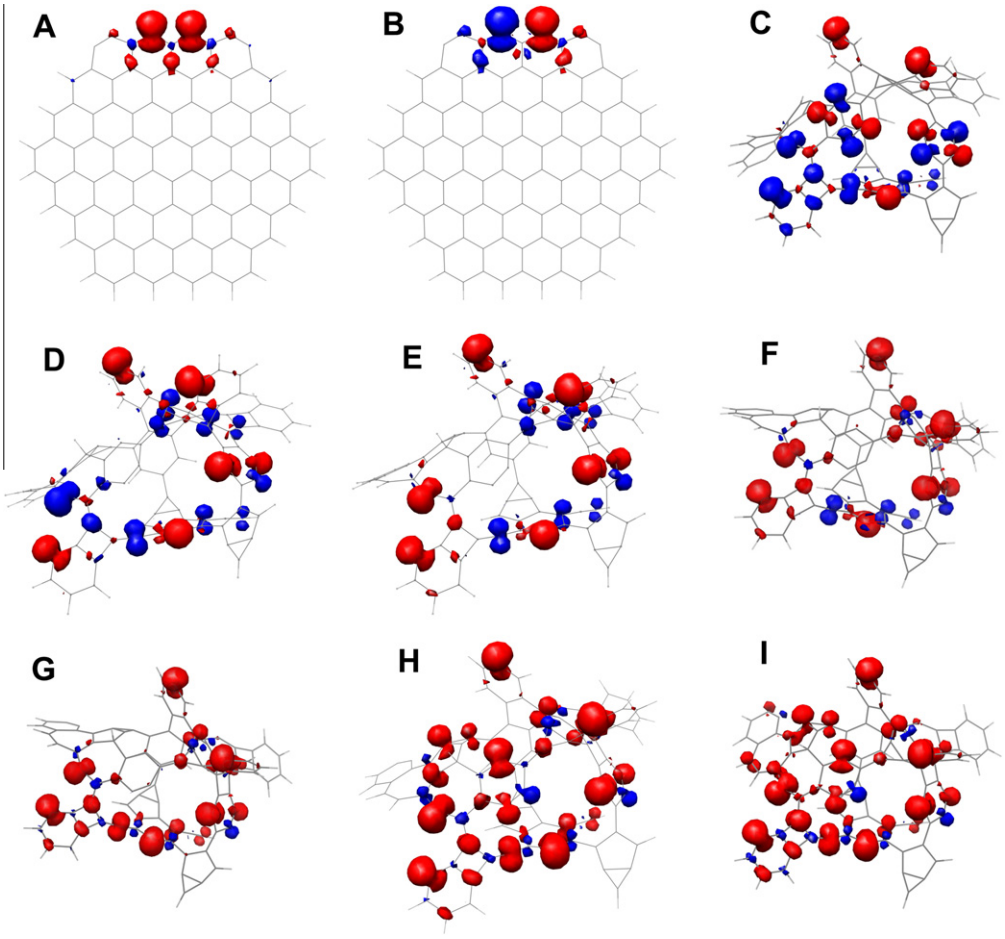

Figure 3. Spin density distribution of (A) the triplet $C_{96}H_{18}$ and (B) the BS singlet $C_{92}H_{24}$ (isosurface level – 0.005) and (C) the BS singlet, (D) the triplet, (E) multiplicity 5, (F) multiplicity 7, (G) multiplicity 9, (H) multiplicity 11, and (I) multiplicity 13 structure **2** (isosurface level – 0.01). The α-spin density is shown in red and the β-spin density in blue. (For interpretation of the references to colour in this figure legend, the reader is referred to the web version of this article.)

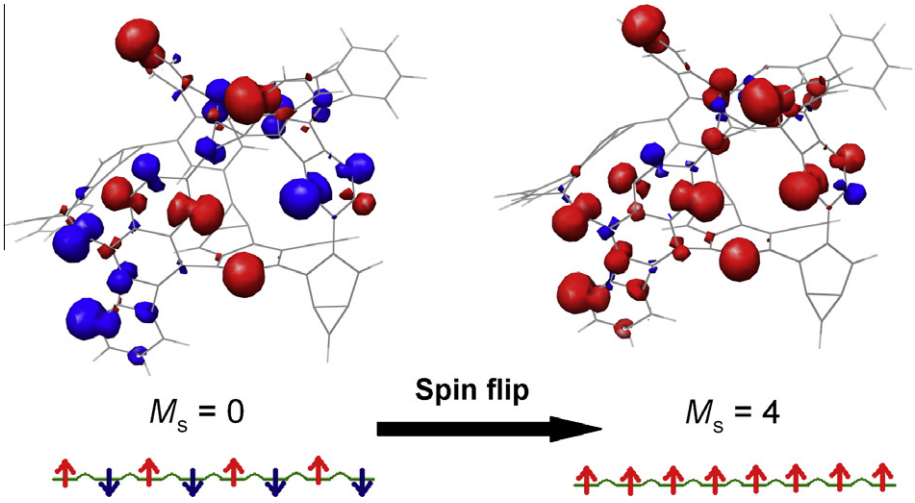

Figure 5. Spin density distribution of the BS singlet and the multiplicity 9 structure **4**. Also shown is a schematic depiction of the spin flip of the electrons in weakly overlapping singly-occupied orbitals that converts the singlet state into the multiplicity 9 state.

(4) benzyne motifs, (5) ordinary aromatic five- and six-membered rings, (6) strained three- and four-membered rings. Only the first type can be characterized as 'strongly' spin-localizing (bearing spin density of at least 0.5), while the second and the third are 'weakly' spin-localizing, in that they bear low spin density. The remaining three types only serve as channels for spin density when included in the conjugation chains. It should be emphasized that the strained three- and four-membered rings bear no spin density and, thus, their highly probable elimination upon thermal relaxation of the amorphous structures should hardly affect the spin properties of the cluster.

The distribution of spin-active centers in structures **2**, **3** and **4** (*cf.* Supplemental Information B) involve different structural elements, but in each case, a fading spin wave is observed around the spin-active centers involving the motifs which act as spin channels. This suggests that the sites that are better conjugated form chains which are responsible for the stabilization of the high-multiplicity states. To prove that point, the electronic structure of an additional cluster, further denoted as **2H**, where one sp^2-hybridized, twofold coordinated, carbon atom of **2** in the middle of the spin chain has been saturated with two H atoms, was calculated in various multiplicity states. As one can see from the data in Table 1, the stabilization of high-multiplicity states vanishes in **2H**, as the RKS and spin-polarized states become essentially iso-energetic. Cleavage of the spin channel also changes the distribution of the spin density drastically, redirecting the chain of spin sites (*cf.* Figure 5). Therefore, the conjugation of spin-active sites in the chain is a key characteristic of the amorphous domain of AC.

A detailed analysis of the electronic structure of the AC cluster models demonstrates that unpaired electrons occupy non-overlapping orbitals within the conjugation chain. In most cases, the overlap of the α- and β-orbitals does not appear to change with spin state. As a result, the energy of the various states is relatively similar for a given range of multiplicities (*e.g.* from the BS singlet to multiplicity 11 for **2** or from the BS singlet to multiplicity 7 for **3**). The latter range of multiplicities over which the states are quasi-degenerate obviously depends on the number of potentially spin-active sites. In fact, unpaired electrons occupy distinct, weakly overlapping, orbitals, forming an antiferromagnetic system, where spin flip can occur without severe energetic penalty (*cf.* Figure 5). Thus, the peculiarity of the graphite-like and amorphous cluster models of AC lies in the high level of conjugation of the electronic system and in the presence of this set of magnetic weakly overlapping atomic orbitals that contribute to the HOMO. Finally, the amorphous domain of AC appears to have semi-metallic properties, being able to change spin state with a negligible energetic penalty within a given range of spin states.

5. Conclusions

The electronic structure of model clusters of the graphite-like and disordered amorphous domains of active carbon (AC), calculated with density-functional theory, suggest a number of interesting features, among which are the stability of high-multiplicity states and the antiferromagnetic nature of the nano-sized domains of AC. It could be of interest to subject the spectroscopic and chemical properties of AC predicted on the basis of this two-domain model to experimental investigation. Conceivably, electron paramagnetic resonance spectroscopy could be used to investigate neat carbon in order to confirm the antiferromagnetic nature of some of its domains. For instance, a combined computational and experimental investigation has recently unveiled the delocalization of spin density on graphene-derived molecular moieties through the characterization of the hyperfine coupling constants of edge protons [46]. However, special techniques may have to be designed to characterize chains of paramagnetic centers, not isolated ones. As a post-polymeric material, AC could also be examined with Raman spectroscopy using the paradigm of defects in conducting polymers [47,48]. Finally, the chemical properties of AC may be reflected in its spin-related reactivity. For instance, interaction with triplet oxygen or reaction with water, as well as other small molecules, might follow different pathways that may not all be spin-conservative. The present results also suggest that spin-catalysis phenomena [49] should be observed over AC. These aspects of the AC spin activity are the subject of on-going work.

Acknowledgments

The authors would like to express their deep gratitude to Prof. M. Ernzerhof (Université de Montreal) for invaluable discussions. This work was partially supported by Concordia University and a Merit Scholarship from the Québec government (Programme de bourses d'excellence pour étudiants étrangers) awarded to OVK. GHP is the recipient of a Concordia University Research Chair. Computational resources were provided by the Centre for Research in Molecular Modeling (CERMM) and by the Réseau Québecois de Calcul Haute Performance (RQCHP). Molecular graphics images

were produced using the UCSF Chimera package from the Resource for Biocomputing, Visualization, and Informatics at the University of California, San Francisco (supported by NIH P41 RR-01081).

Appendix A. Supplementary data

Supplementary data associated with this article can be found, in the online version, at doi:10.1016/j.cplett.2011.08.009.

References

[1] R.E. Franklin, Proc. R. Soc. London, A 209 (1951) 196.
[2] H. Marsh, F. Rodríguez-Reinoso, Activated Carbon, Elsevier, London, 2006.
[3] B.E. Warren, Phys. Rev. 9 (1934) 551.
[4] B.E. Warren, Phys. Rev. 59 (1941) 693.
[5] P.J.F. Harris, Crit. Rev. Solid State Mater. Sci. 30 (2005) 235.
[6] P.J.F. Harris, Phil. Mag. 84 (2004) 3159.
[7] K. László, K. Josepovits, E. Tombácz, Anal. Sci. 17 (suppl.) (2001) i1741.
[8] A. Braun et al., Combust. Flame 137 (2004) 63.
[9] X. Li, L. Liu, S. Shen, Carbon 39 (2001) 2335.
[10] P.J.F. Harris, in: K.H.J. Buschow, R.W. Cahn, M.C. Flemings, B. Ilschner, E.J. Kramer, S. Mahajan (Eds.), The Encyclopedia of Materials: Science and Technology, vol. 6, Elsevier, Amsterdam, New York, 2001, p. 6197.
[11] S. Ergun, Carbon 6 (1968) 141.
[12] J. Rodriguez, F. Ruette, J. Laine, Carbon 32 (1994) 1536.
[13] N. Kojima, T. Ohba, Y. Urabe, H. Kanoh, K. Kaneko, J. Nanomater. (2011) 853989-1.
[14] A.P. Terzyk, S. Furmaniak, P.A. Gauden, P.J.F. Harris, J. Włoch, P. Kowalczyk, J. Phys.: Condens. Matter 19 (2007) 406208.
[15] A.P. Terzyk, S. Furmaniak, P.J.F. Harris, P.A. Gauden, J. Włoch, P. Kowalczyk, G. Rychlicki, Phys. Chem. Chem. Phys. 9 (2007) 5919.
[16] V.D. Khavryuchenko, O.V. Khavryuchenko, A.I. Shkilnyy, D.A. Stratiichuk, V.V. Lisnyak, Materials 2 (2009) 1239.
[17] J.W. Neely, US Patent No. 4040,990 (1977).
[18] H. Von Blucher, E. De Ruiter, US Patent No. 5977,016 (1999).
[19] A.M. Puziy, Langmuir 11 (1995) 543.
[20] V.D. Khavryuchenko, O.V. Khavryuchenko, V.V. Lisnyak, Chem. Phys. 368 (2010) 83.
[21] I. Zilberberg, S.Ph. Ruzankin, Chem. Phys. Lett. 394 (2004) 165.
[22] V.D. Khavryuchenko, Y.A. Tarasenko, V.V. Strelko, O.V. Khavryuchenko, V.V. Lisnyak, Int. J. Mod. Phys. B 21 (2007) 4507.
[23] V.D. Khavryuchenko, O.V. Khavryuchenko, Y.A. Tarasenko, V.V. Lisnyak, Chem. Phys. 352 (2008) 231.
[24] M.R. Philpott, F. Cimpoesu, Y. Kawazoe, Mater. Trans. 49 (2008) 2448.
[25] M.R. Philpott, F. Cimpoesu, Y. Kawazoe, Chem. Phys. 354 (2008) 1.
[26] A.D. Becke, J. Chem. Phys. 98 (1993) 5648.
[27] F. Neese (2009) ORCA 2.7.0. <http://www.mpi-muelheim.mpg.de/bac/logins/downloads_en.php>.
[28] A. Schaefer, H. Horn, R. Ahlrichs, J. Chem. Phys. 97 (1992) 2571.
[29] A.D. Becke, Phys. Rev. A 38 (1988) 3098.
[30] J.P. Perdew, Phys. Rev. B 33 (1986) 8822.
[31] F. Weigend, R. Ahlrichs, Phys. Chem. Chem. Phys. 7 (2005) 3297.
[32] E.F. Pettersen, T.D. Goddard, C.C. Huang, G.S. Couch, D.M. Greenblatt, E.C. Meng, T.E. Ferrin, J. Comput. Chem. 25 (2004) 1605.
[33] V.D. Khavryuchenko, O.V. Khavryuchenko, Yu.A. Tarasenko, A. Shkilnyy, D. Stratiichuk, V.V. Lisnyak, Int. J. Mod. Phys. B 24 (2010) 1449.
[34] J.J.P. Stewart, J. Comput. Chem. 10 (1989) 209.
[35] J.J.P. Stewart, J. Comput. Chem. 10 (1989) 221.
[36] R. Ditchfield, W.J. Hehre, J.A. Pople, J. Chem. Phys. 54 (1971) 724.
[37] W.J. Hehre, R. Ditchfield, J.A. Pople, J. Chem. Phys. 56 (1972) 2257.
[38] I.G. Kaplan, J. Mol. Struct. (Theochem) 838 (2007) 39.
[39] J.H. Rodriguez, J.K. McCusker, J. Chem. Phys. 116 (2002) 6253.
[40] M. Atanasov, B. Delley, F. Neese, P.L. Tregenna-Piggott, M. Sigrist, Inorg. Chem. 50 (2011) 2112.
[41] F. Neese, J. Phys. Chem. Solids 65 (2004) 781.
[42] L. Noodleman, J. Chem. Phys. 74 (1981) 5737.
[43] L. Noodleman, E.R. Davidson, Chem. Phys. 109 (1986) 131.
[44] K.E. Edgecombe, A.D. Becke, Chem. Phys. Lett. 244 (1995) 427.
[45] C. Liu, S-Y. Chung, S. Lee, S. Weiss, D. Neuhauser, J. Chem. Phys. 131 (2009) 174705.
[46] Y. Morita, S. Suzuki, K. Sato, T. Takui, Nat. Chem. 3 (2011) 197.
[47] G. Messina, S. Santangelo (Eds.), Carbon: The Future Material for Advanced Technology Applications, vol. 100, Topics Appl. Phys., Springer, Berlin, Heidelberg, 2006.
[48] F. Cataldo (Ed.), Polyynes: Synthesis, Properties, and Applications, CRC Press, Boca Raton, 2006.
[49] V.D. Khavryuchenko, O.V. Khavryuchenko, V.V. Lisnyak, Catal. Commun. 11 (2010) 340.